International Journal of Pharmaceutics: X 1 (2019) 100013

Contents lists available at ScienceDirect

International Journal of Pharmaceutics: X

journal homepage: www.journals.elsevier.com/international-journal-of-pharmaceutics-x

Development of a novel method utilising dissolution imaging for the measurement of swelling behaviour in hydrophilic matrices

Adam Ward[a], Karl Walton[b], Nihad Mawla[a], Waseem Kaialy[c], Lande Liu[d], Peter Timmins[a], Barbara R. Conway[a], Kofi Asare-Addo[a,*]

[a] Department of Pharmacy, University of Huddersfield, Huddersfield HD1 3DH, UK
[b] EPSRC Future Metrology Hub, University of Huddersfield, Huddersfield HD1 3DH, UK
[c] School of Pharmacy, University of Wolverhampton, Faculty of Science and Engineering, Wolverhampton WV1 1LY, UK
[d] Department of Chemistry, University of Huddersfield, Huddersfield HD1 3DH, UK

ARTICLE INFO

Keywords:
HPMC
Hypromellose
Surface dissolution imaging
Swelling

ABSTRACT

A variety of imaging techniques are currently used within the field of pharmaceutics to help understand and determine a wide range of phenomena associated with drug release from hydrophilic matrix tablets. This work for the first time aims at developing an appropriate testing imaging methodology using a surface dissolution imaging instrument (SDI2) for determining the swelling of whole compacts using hypromellose as a model hydrophilic matrix former. The influence of particle morphology (CR and DC grades) and two compressional forces (5 and 15 kN) on the initial swelling behaviour of hypromellose were investigated. The results showed that a lower absorbance of 50 mAu with a wider measurement zone proved successful in determining the edge of the gel layer and growth measurements in real-time with high level of details under flow. Despite the differences in the morphology of the grades of hypromellose tested, it was however discovered that gel growth was statistically similar between them which may be attributed to their similar chemistry. This novel method also highlighted differences in the hydrated polymer's appearance which may have been as a result of differences in porosity and solid fraction. This information is of great importance to a formulator as gel growth plays a crucial role in determining drug release from polymer compacts.

1. Introduction

Hypromellose, also known as hydroxypropyl methylcellulose (HPMC), is a commonly used cellulose ether found in many pharmaceutical formulations and used frequently in the formulation of hydrophilic matrices. Hypromellose is a water soluble, hydrophilic, non-ionic cellulose ether that gels, which is stable over the pH range of 3 to 11 and is enzyme resistant. The use of hypromellose in tablet formulations allows for the extended release of a drug to prolong its therapeutic effect (Siepmann et al., 2017; Asare-Addo et al., 2013a; Nokhodchi et al., 2012; Li et al., 2005). Due to the extensive use of hypromellose within the pharmaceutical industry, the polymer is well characterised, with studies focusing on the influence of initial dissolution (Campos-Aldrete and Villafuerte-Robles, 1997), particle size (Heng et al., 2001), morphology on drug release (Bonferoni et al., 1996). Better mechanistic understanding of factors associated with performance of hypromellose in extended release hydrophilic matrix tablets will contribute to a robust quality-by-design approach to these products (Timmins et al., 2016).

Amongst the wide range of hypromellose grades available, the high molecular weight hypromellose 2208 is the most widely used in ER matrix formulations (Asare-Addo et al., 2013b). Hypromellose 2208 can be used for wet and dry granulation in controlled release applications (Levina and Rajabi-Siahboomi, 2014) in polymer combinations (Hu et al., 2017) and 3D printed dosage forms (Khaled et al., 2015). Following on from the availability of the CR grade of hypromellose 2208, DC2 is a new addition to the polymers supplied by the Dow Chemical Company and will herewith be referred to as DC in the manuscript. The DC grade is designed to offer the same performance and reliability as the CR grade. The DC grade was compared recently to its CR equivalent and the results concluded that the DC2 grade did flow better than its CR counterpart. Tablets produced to a standard porosity also provided

Abbreviations: HPMC, hydroxypropyl methyl cellulose; SDI, surface dissolution imaging; SEM, scanning electron microscope; NIR, near infra-red; MRI, magnetic resonance; NMR, nuclear magnetic resonance; CLSM, confocal laser scanning microscopy

* Corresponding author.
E-mail address: k.asare-addo@hud.ac.uk (K. Asare-Addo).

https://doi.org/10.1016/j.ijpx.2019.100013
Received 5 November 2018; Received in revised form 3 April 2019; Accepted 8 April 2019
Available online 10 April 2019

similar strength tablets (Van Snick et al., 2017). A similar comparative study also concluded that the CR grade controls the release rate of ibuprofen better than the DC grade (Ervasti et al., 2015). There are however no studies that have explored how the engineered particles of these polymers can influence early hydration and swelling properties, a key property in the establishment of drug release from hydrophilic matrices (Timmins et al., 2014).

A variety of imaging techniques are currently used within the field of pharmaceutics to help understand and determine a wide range of phenomena associated with drug release from hydrophilic matrix tablets. These imaging techniques include near Infra-red (NIR), Magnetic Resonance (MRI), Nuclear Magnetic Resonance (NMR), Terahertz, and Confocal laser scanning microscopy (CLSM). NIR has been used to monitor the development of the gel layer formed in compacts containing HPMC (Avalle et al., 2011) as well as monitoring drug release as a result of erosion (Avalle et al., 2013). MRI has been implemented to monitor the movement of water in pastes (Tomer et al., 1999), model polymer dissolution (Kaunisto et al., 2010), visualize *in vivo* tablet dissolution (Christmann et al., 1997) and to monitor the structural evolution of hypromellose tablets (Kulinowski et al., 2011). A novel imaging application using NMR was also developed and used to monitor water front penetration (Ashraf et al., 1994), water mobility and drug diffusion in hydrophilic matrices (Rajabi-Siahboomi et al., 1996) and drug diffusion in hydrogels (Dinarvand et al., 1995). Terahertz pulsed imaging has been used to monitor the swelling and drug diffusion of tablets containing HPMC (Markl et al., 2018; Yassin et al., 2015) whilst a review has been conducted into the suitability of the tool for characterizing film coating (Haaser et al., 2013). Confocal laser scanning microscopy (CLSM) has also been utilised in a variety of pharmaceutical applications (Pygall et al., 2007). Key related applications include the measurement of the surface roughness of tablets (Peltonen et al., 1997), monitoring gel layer growth and water penetration in hydrophilic matrices (Melia et al., 1997) and surface profilometry of dissolving tablet surfaces (Healy et al., 1995).

UV dissolution imaging, has already begun to prove its versatility within pharmaceutics. The primary use of the technique (surface dissolution imaging, SDI) is to obtain intrinsic dissolution rates of pharmaceutical ingredients (Ward et al., 2017; Boetker et al., 2013). However, the technique has begun to diversify into an analytical tool for the monitoring of a variety of dissolution events. These can be events with API (Asare-Addo et al., 2019, 2018; Hulse et al., 2012), release from transdermal patches (Østergaard et al., 2010) or the dissolution behaviour of polymers (Pajander et al., 2012). The model of the surface dissolution imaging instrument employed in this work allows imaging of whole dosage forms in real time due to the addition of a whole dosage flow cell. The SDI2, an upgrade on its predecessor, has a number of new key features and updates. The first relates to the optics used in the system. The SDI2 has the ability to record UV data at 2 wavelengths simultaneously with wider range of wavelengths available (255, 280, 300 and 320 nm). This is also accompanied by an additional wavelength of 520 nm to record any events at a visible wavelength (Sirius Analytical, 2017). The next update relates to the flow cell used in the system. The work reported here uses this novel system to provide all imaging data.

The following work is aimed at taking advantage of the novel whole dosage cell supplied with the SDI2 instrumentation and the use of the additional 520 nm LED to image the initial stages of gel formation within hydrophilic matrix systems. This work also looks to build upon previous HPMC work described by Pajander et al. (2012) where swelling behaviour was studied from a single surface of a 3 mm compact (~5 mg). In this work, a method is developed that allows the swelling characteristics of a whole dosage form (250 mg compact) in situ to be studied, whilst also taking advantage of the larger imaging area and higher resolution available in the SDI2 system. This developed methodology was further explored to determine its suitability in differentiating between the same polymer with different morphologies. To date, there has not been any work investigating the use of the second generation dissolution imaging instrument (SDI2) to provide such a unique insight.

2. Material and methods

2.1. Materials

Methocel HPMC K100M CR grade and HPMC DC2 grade were kind donations from Colorcon Ltd, UK. These polymers are referred to CR and DC respectively throughout the manuscript. Deionised water was used for the swelling analysis.

3. Methods

3.1. Scanning electron microscopy (SEM)

Electron micrographs were obtained on Jeol JSM-6060CV SEM instrument operating at 20 kV as described previously in Asare-Addo et al. (2015). Briefly, the samples were mounted on a metal stub with double-sided adhesive tape and were sputter-coated with an ultra-thin coating of gold/palladium (80:20) for 60 s using a Quorum SC7620 Sputter Coater under vacuum with gold in an argon atmosphere prior to observation. Micrographs with different magnifications were taken to facilitate the study of the morphology of the hypromellose particles.

3.2. Laser diffraction

Volume-weighted particle size analysis were conducted using a Malvern Mastersizer 2000 (Malvern Instruments Ltd, Germany) laser diffraction particle size analyser equipped with a dry sampling system (Aero S, Malvern Instruments, UK) which is able to characterise over the particle size range from 0.1 µm to 3500 µm. Before measurement, a background reading was taken. The dispersion of air pressure was adjusted to 2.0–bar, and a feed rate of 30% was applied. The measurement time was 5 s. The particle sizes at 10% ($d_{10\%}$), 50% ($d_{50\%}$, median diameter) and 90% ($d_{90\%}$) of the volume distribution, and the volume mean diameter (VMD, the average diameter based on the unit volume of a particle) were calculated automatically using the Malvern Software (version 2.20). The span of the volume distribution was used as a measure of the width of the distribution of size relative to the median diameter. Three samples were measured for each product and results were averaged.

3.3. Tablet manufacture and hardness determination

Flat faced 8 mm diameter round polymer compacts (CR and DC) of target weight 250 mg were made using a 10 station automated tabletting machine (Riva, Argentina) at a compression force of 5 and 15 kN. The porosity (calculated using Eq. 1) and solid fractions of the CR and DC tablets at the different compression forces were determined (mean of three determinations). The true density of the polymers was determined using the Micromeritics Accupyc II pycnometer 100 (Micromeritics, USA).

$$Tabletporosity = \left[1 - \left[\frac{tabletweight/tabletvolume}{truedensityofpowder}\right]\right] X100 \quad (1)$$

The compressed polymer compacts were fractured diametrically using the Pharmatest hardness tester (Germany) (n = 10 tablets) after 48 h.

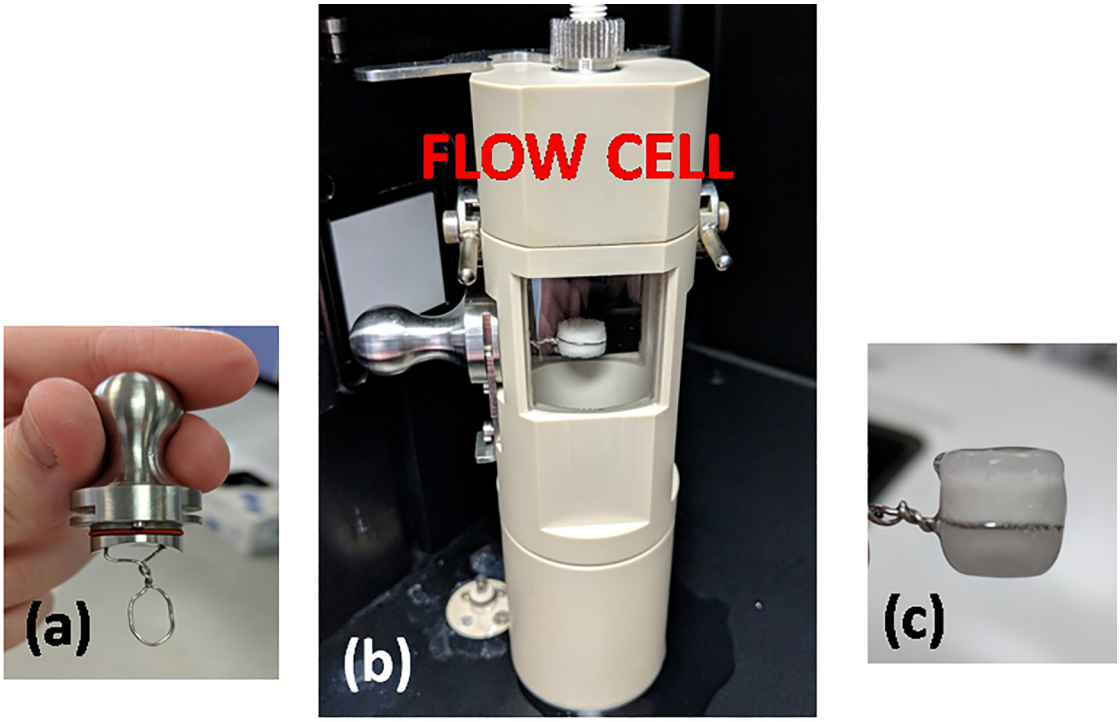

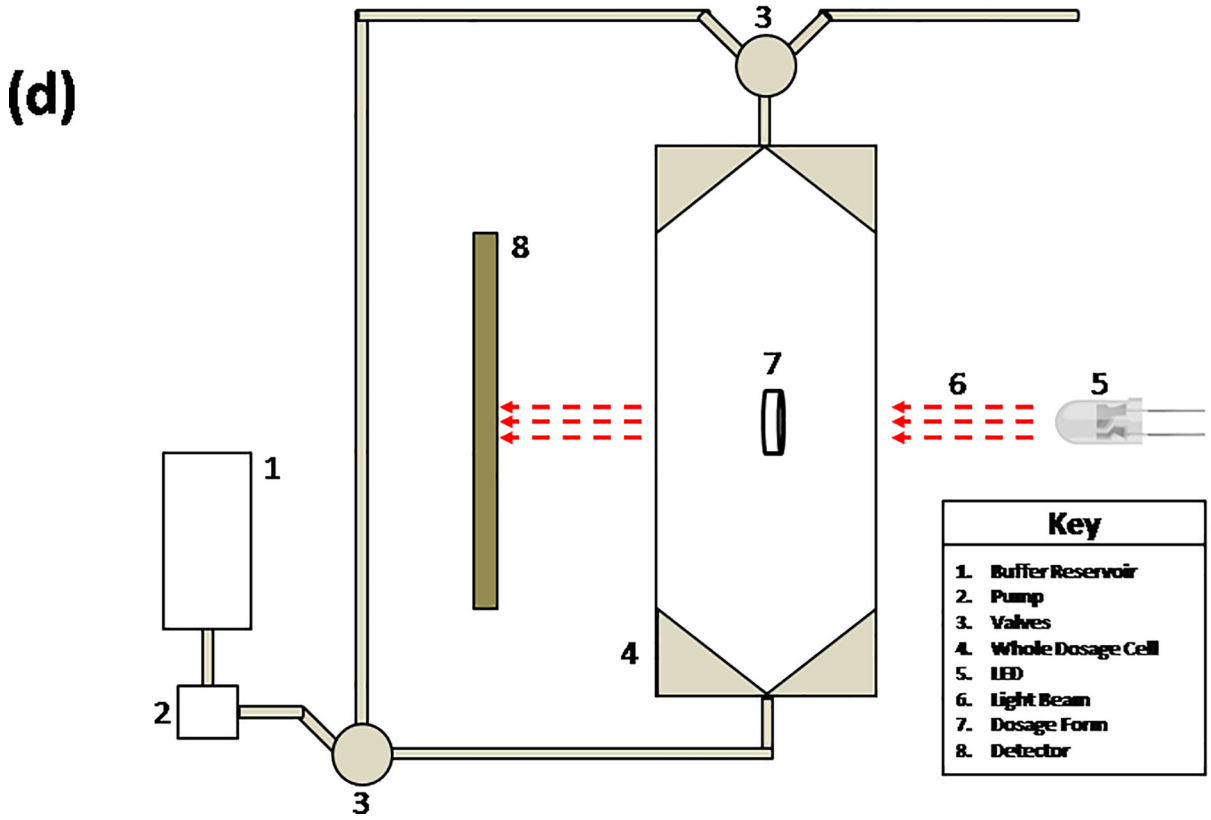

Fig. 1. (a) Image of wire tablet holder designed for holding the tablet for swelling studies, (b) tablet holder inserted into the flow cell for image analysis, (c) image of swollen tablet after data acquisition in flow cell of SDI2 instrument, (d) schematic representation of the surface dissolution imaging instrument (SDI2) with key inserted in figure.

3.4. Surface dissolution imaging, SDI2

3.4.1. SDI2 imaging method development of swelling in CR and DC compacts

Before data collection, a tablet was placed in a wire tablet holder (Fig. 1a). Next, borosilicate beads were added to the whole dosage flow cell such that they covered the one-way valve and evenly covered the bottom third of the flow cell (approximately 12.3 g). The whole dosage cell was inserted into the system and connected to the fluid lines before being locked in place. The system was then set to run a flush cycle to clean the pumps, lines and the cell. Deionized water was used as the cleaning solution. Once the flush program had completed an experiment was set up with the following specifications; Dissolution specifics: open loop, whole dosage, single solution; Experiment length: 2 h; Media: deionized water (pH 5); Flow rate: 8 mL/min; Temperature: 37 °C; Wavelength: Dual wavelengths at 520 nm. 3 polymer compacts per grade and compression force giving a total of 12 compacts (6 CR compacts at 5 kN and at 15 kN; 6 DC compacts at 5 kN, and at 15 kN) were analysed.

The flow cell was filled with approximately 70 mL of deionised water before reducing it to approximately 30 mL. At this point, data collection was paused to allow for sample insertion. The wire holder containing the tablet was inserted into a removable stainless steel seal situated on the side of the flow cell and placed into the flow cell. Care was taken to ensure that no water came into contact with the tablet surface. The experiment was restarted and data collection resumed as the whole dosage cell (Fig. 1b) filled with the deionised water.

Once the experiment was complete, the cell was drained and the flow cell removed. The tablet was removed from the flow cell and wire holder (Fig. 1c) and discarded. The beads were emptied from the cell into a glass beaker and rinsed with de-ionised water and isopropanol before being emptied onto paper towels to air dry. The cell and wire holder were cleaned with isopropanol and de-ionised water and dried using paper towels. Once all components were dry the whole dosage cell was re-assembled and placed back into the system ready for the next experiment. The schematic of the SDI2 is depicted in Fig. 1d.

3.4.2. Data analysis

The data files from the data collection were analyzed using a bespoke software (Sirius Analytical Ltd) tailored for the SDI2 system. To determine the increase in the tablets axial growth, each dry tablet at the three compaction levels for each polymer compact was normalized to 0 mm. The dissolution footage was edited to display using the 'jet' colour scheme and exported in '.wmv' format for further analysis (observing the tracking box).

3.4.3. Effect of tablet measurement zones

The current methodology as discussed in Section 2.6.1 yielded results as indicated in Supplementary figure (S1). S1a, displays how the measurement zones are located centrally to the tablet with a narrow thickness of 0.5 mm and also how the tracking box follows the edge of the tablet based on an absorbance threshold (500 mAu). However, during initial analysis of the polymer compacts, a significant flaw with this methodology was discovered. It appeared that as gel growth progressed, and the gel layer began to form, the tracking box responsible for the height and width measurements appeared to lose track of the edge of the gel layer thereby producing erroneous results (**S1**b). As a result, different zones as indicated in Supplementary figure (S2) a and b were investigated at the 500 mAu threshold to determine if the movement of the measurement zones had an effect on the ability of the tracking box to trace the edge of the gel layer accurately.

3.4.4. Effect of tablet threshold measurements

The same methodology detailed in section 2.6.1 was used in the development of tablet threshold measurements. As indicated in S1b, initial data obtained at the 500 mAu threshold suggested that a significant amount of gel growth was not tracked. As a result, several experiment were conducted at various absorbance thresholds (25, 50, 75, 100, 150, 350 and 500 mAu) to determine the appropriate threshold to use for these hydrophilic matrices.

3.4.5. Effect of flow rate

Section 2.6.1 was used again in the development of this method with the only difference being the change in flow rate. In these set of experiments, flow rate was varied at 4, 8 and 16 mL/min to mimic low, medium and high flow rates in the SDI2 instrument.

4. Results and discussion

4.1. Physical properties of the CR and DC grades

Laser diffraction analysis showed CR ($D_{10\%}$ 30.9 ± 1.0 μm, $D_{50\%}$ 87.5 ± 2.6 μm, $D_{90\%}$ 217.0 ± 6.9 μm, VMD 108.0 ± 3.5 μm and Span 2.1 ± 0.1) to have smaller particle size distribution compared to DC ($D_{10\%}$ 50.0 ± 2.5 μm, $D_{50\%}$ 125.0 ± 4.6 μm, $D_{90\%}$ 268.0 ± 5.0 μm, VMD 144.7 ± 4.0 μm and Span 1.7 ± 0.1). This is substantiated by SEM photographs (Supplementary Fig. (S3)). The SEM images also showed the CR and DC grades to have different particle shapes. The CR grade contained a mixture of fibrous and irregularly shaped particles. This agreed with previous observations previously reported (Van Snick et al., 2017). The DC grade however had rounder and agglomerated particles which along with their larger size distribution, suggest that they have better flow than the CR grade. The true density values for the CR and DC grades were 1.3174 ± 0.004 g/cm^3 and 1.3239 ± 0.001 g/cm^3 respectively. It was interesting to note that the differences in morphology impacted on the tablet porosity and solid fraction for all the samples at the different compactions studied (5 and 15 kN) (Table 1). DC had the highest tablet porosity when compared to that of the CR grade at all the different compactions studied (Table 1). For both the CR and DC samples, there was a general decrease in porosity and therefore an increase in their solid fraction with an increase in the compressional forces they were subjected to. This relatively higher porosity in the DC samples as well as their relatively lower solid fraction to their CR counterpart may impact on their rate of water ingress. Table 1 also shows that despite the differences discussed above, in regards to the mechanical strength of the tablets, both the CR and DC grade compacts had similar values at the same compaction forces used (Table 1) with the DC grade having a smaller standard deviation value each time. It was also observed that there was an increase in mechanical strength with increase compaction for all the samples (Table 1).

4.2. SDI2 method development results

4.2.1. Effect of measurement zones, tablet threshold and flow rate

Tracking the height and width of the compact during the swelling relied on two key inputs; the location of the horizontal and vertical zones and the tablet edge threshold absorbance. A 5 kN DC compact was initially used to test the influence of tablet edge threshold and location of the measurement zone. An investigation of the influence of the measurement zone location on the gel growth measurement using 3 locations labelled A, B and C (Fig. 2a) using the tablet edge threshold at

Table 1
Summary of hypromellose CR and DC polymer compact properties used in the study.

	Porosity (%)	Solid fraction* (%)	Tablet hardness (N)	Tablet height (mm)
5kN CR	15.3 ± 1.8	84.7 ± 1.8	123.1 ± 18.9	3.95 ± 0.10
15kN CR	11.3 ± 0.6	88.7 ± 0.6	193.3 ± 12.4	4.49 ± 0.02
5kN DC	25.1 ± 0.8	74.9 ± 0.8	122.6 ± 3.9	3.91 ± 0.06
15KN DC	18.6 ± 1.8	81.4 ± 1.8	188.4 ± 10.5	4.22 ± 0.25

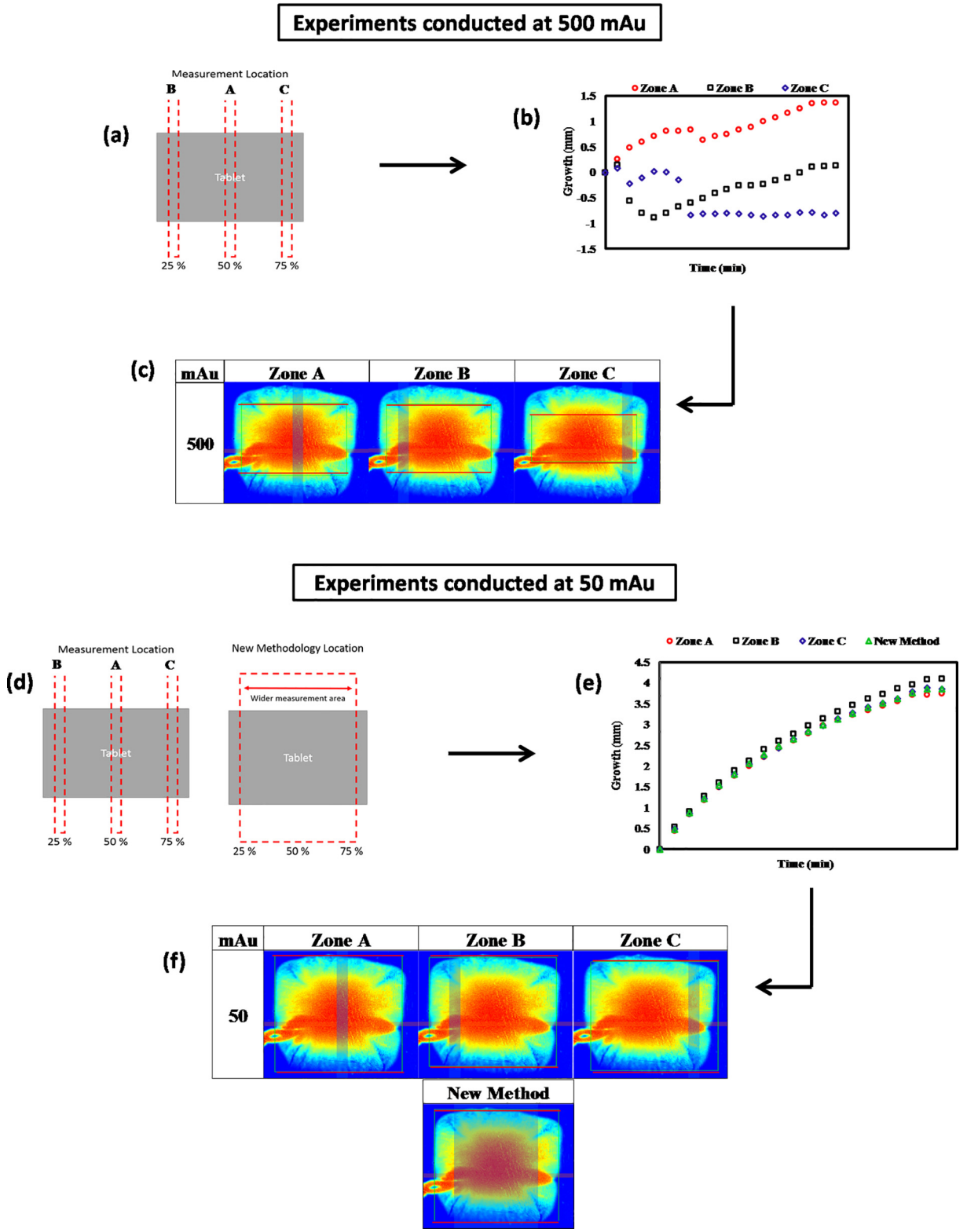

Fig. 2. (a) Measurement locations in determining appropriate place in measuring tablet edge threshold, (b) Gel growth measurements using measurement zones from Fig. 2a, (c) False coloured SDI2 images of experiments conducted at an absorbance threshold of 500 mAu. Red lines show where the tracking box is measuring the "gel layer" at the selected zones in Fig. 2a causing the erroneous readings in Fig. 2b, (d) Measurement location for newly developed methodology and measurement locations from Fig. 2a now using a lower absorbance threshold of 50 mAu, (e) Gel growth measurements using measurement zones from Fig. 2d showing how new method with wider measurement area compares to the zonal measurements with new absorbance of 50 mAu, (f) False coloured SDI2 images of experiments conducted at an absorbance threshold of 50 mAu. Red lines show where the tracking box is measuring the "gel layer" at the selected zones in Fig. 2d and staying true to the gel layer edge to produce readings in Fig. 2e. (For interpretation of the references to colour in this figure legend, the reader is referred to the web version of this article.)

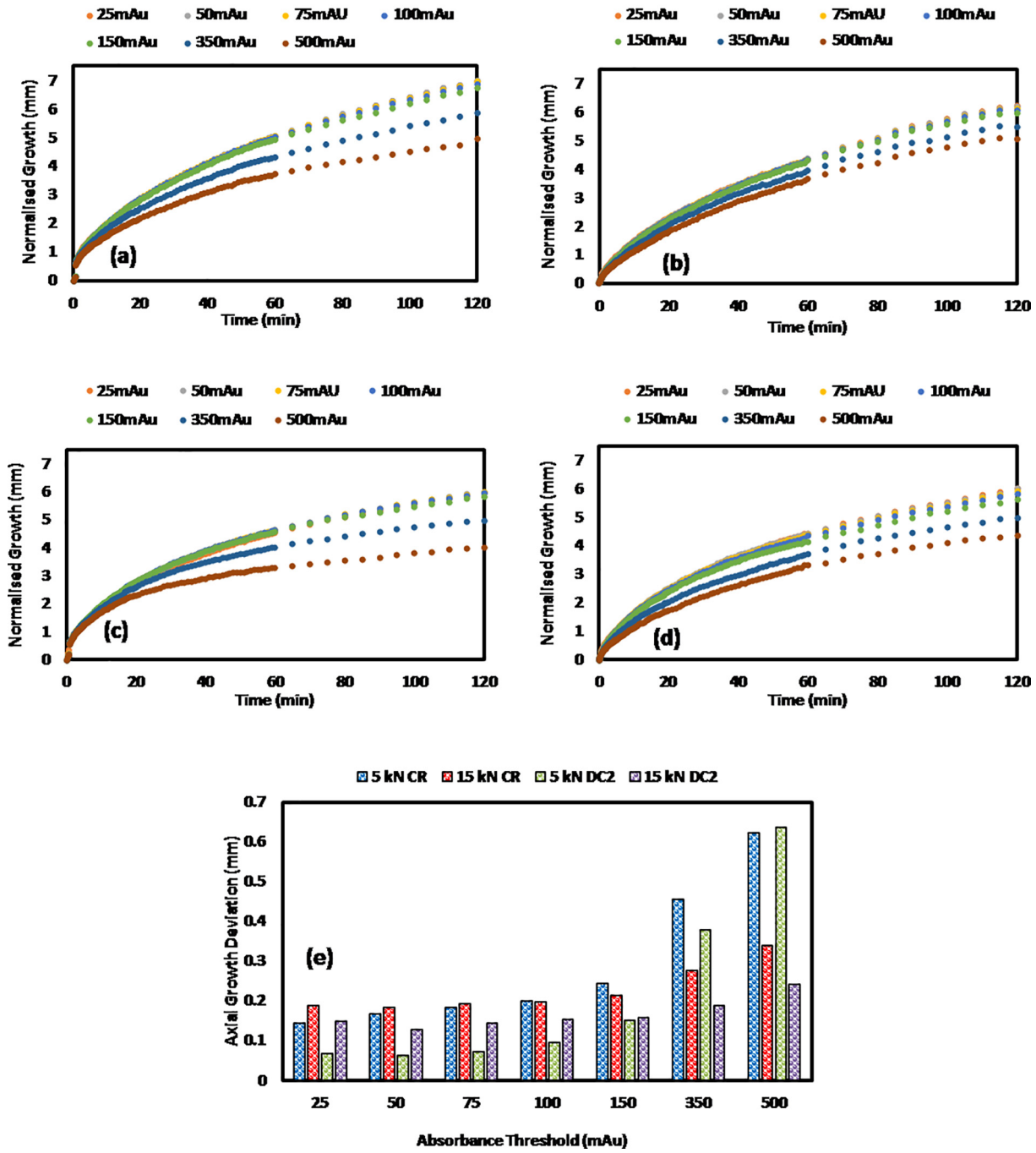

Fig. 3. Normalised gel layer growth measurement at absorbance thresholds of 25, 50, 75, 100, 150, 350 and 500 mAu for (a) 5 kN CR, (b) 15 kN CR, (c) 5 kN DC, (d) 15 kN DC, (e) The average deviation for all the absorbance thresholds tested for both CR and DC at 5 and 15 kN.

500 mAu showed that both the location of the measurement zones and the threshold absorbance of 500 mAu produced un-reliable growth measurements (Fig. 2b). Fig. 2c shows where the tracker picked the axial gel growth lines from in generating Fig. 2b (highlighted red lines). It was therefore necessary to develop a new methodology that allowed for accurate gel layer and growth detection and measurements. A lower absorbance **threshold** of 50 mAu was thus investigated further with a wider zone that measured the complete center portion of the tablet starting at location B and ending at C (Fig. 2d-labelled the new methodology location). The use of the lower absorbance threshold of 50 mAu was a success at the tested measurement locations B and ending at C as well as the new wider zone location (Fig. 2e). Fig. 2f shows where the tracker picked the axial gel growth lines from in generating Fig. 2e (highlighted red lines). Over the course of the 2 h swelling experiment, the tracking box used to provide height and width measurements stayed true to the edge of the gel layer. The use of the new wider zone was as such far more robust and capable of monitoring gel growth accurately as the shape of the gel growth began to become more apparent towards the latter stages of the swelling experiment.

Investigations were further conducted to determine if robust measurements could also be obtained at several absorbance thresholds. The normalized gel growths for the CR and DC polymers at the 5 and 15 kN compacts are depicted in Fig. 3a-d with their deviations in Fig. 3e. The graphs in Fig. 3 suggest absorbance thresholds of 25–150 mAu

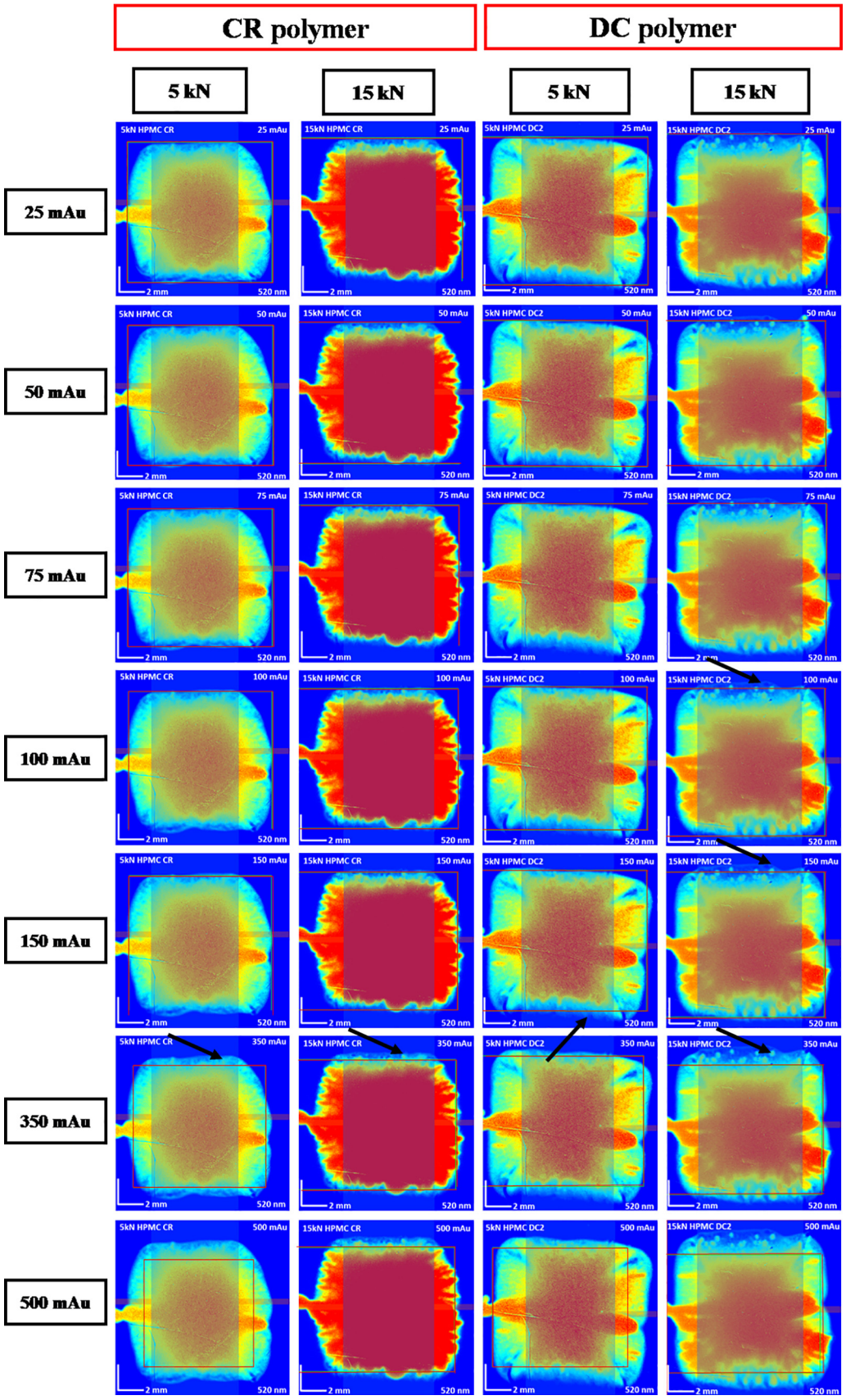

Fig. 4. False coloured SDI2 images for polymer compacts obtained from the SDI2 instrument at absorbance thresholds of 25, 50, 75, 100, 150, 350 and 500 mAu for both the CR and DC polymer compacts at 5 and 15 kN. Note: The black arrows here indicate parts of the "gel layer" that had not been taken into account by the measurement box.

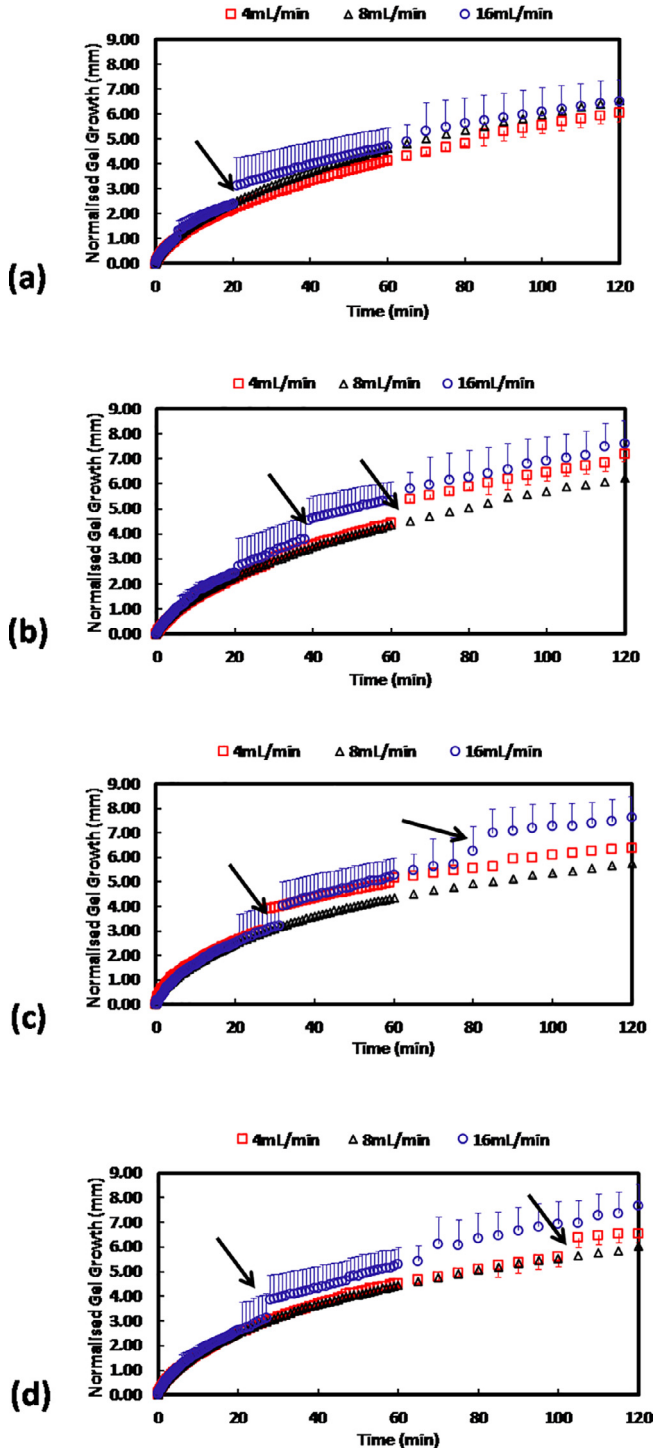

Fig. 5. Normalised gel layer growth measurement at the absorbance thresholds of 50 mAu for (a) 5 kN CR, (b) 15 kN CR, (c) 5 kN DC, (d) 15 kN DC at flow rates of 4, 8 and 16 mL/min. Note: The black arrows here indicate air bubbles lodged next to the compacts potentially giving erroneous results which is observed as "jumps" in the normalised gel growth.

produced similar normalized gel growths. The 350 and 500 mAu thresholds however, had higher deviations suggesting that those thresholds were not suitable for the polymers tested. It was however interesting to note from the corresponding images in Fig. 4 that some of the gel measurements were also missed by the tracking box (red box around compact in determining axial growth) (gel layers missed highlighted by a black arrow) even at the absorbance thresholds of 100 and 150 mAu.

The flow rate results are depicted in Figs. 5 and 6. Fig. 5 shows the effect of the flow rate on the normalized gel growth of the CR and DC compacts at 5 and 15 kN. The flow rate at 16 mL/min seemed quite turbulent and as a result often lodged bubbles next to the compacts (indicated by the black arrows on Fig. 6) that gave erroneous results. This can be observed as the jumps in the normalized gel growth in Fig. 5 (highlighted by the black arrows). This **da**ta suggested that the gel layer growing extensively at this higher flow rate was false as visual inspection showed the higher flow rate to disrupt the gel layer. It would therefore be interesting to study the influence of fluid dynamics on dosage forms (also effect of possible orientation). It is however important to bear in mind that the SDI2 instrument is designed for small scale dissolution studies to aid preformulation studies. As such the large volume needed in conducting the studies at 16 mL/min is unwarranted. The flow rates of 4 mL/min and 8 mL/min worked well in determining the gel growth of the CR and DC compacts with the later proving extremely consistent with both polymers and at both 5 and 15 kN.

4.3. Swelling analysis of CR and DC compacts

An $n = 3$ experiment was conducted on both the CR and DC polymers at each compaction level. The time points selected for the images were 1, 2, 5, 20, 30, 60, 90 and 120 min. Based on the method development, an absorbance threshold of 50 mAu, a wider measurement zone and a flow rate of 8 mL/min were selected for these set of experiments. The SDI2 images depicted in Fig. 7 highlight the subtle but important differences in the initiation of the formation of the gel layer between the two polymers at the different compaction levels. The system also produced a real-time swelling video that allowed for further insight into the behaviour of the compacts. The swelling plot shown in Fig. 8, highlights the differences between the two polymers at the different compaction levels over the course of the experiment. Pajander et al. 2012 investigated the behaviour of two different grades of hypromellose using an Actipix SDI300 dissolution imaging system (Paraytec Ltd., York, United Kingdom) with an Actipix flow-through dissolution cartridge CADISS-2. The authors found the different polymers to behave similarly with regards to swelling, gelling and erosion at the compacts surface. Kavanagh and Corrigan., 2004 studied a range of different molecular weighted HPMC polymers and observed that the change in weight which reflected swelling for the higher molecular weight polymers (HPMC K100M) had the highest maximum swelling over a 12 h period with very little erosion occurring. These polymers also showed the highest dissolution medium uptake. Table 1 shows the initial compact heights used for the imaging analysis. From Fig. 8, where the initial heights were normalised, it can be observed that the compacts had imbibed the media and swollen to ~6–7 mm in just 2 h reflecting Kavanagh and Corrigan's observations.

An independent sample *t*-test with equal variances was used to test the statistical significance of the difference between the two polymers at the different compaction levels. The null hypothesis was that the profiles were the same using a 95% confidence interval. The results were that the null hypothesis could be retained for all the profiles over the 0–120 min range. There was however a statistical difference between the 5 kN CR vs. DC which was detected between 60 and 120 min ($p = 0.007$).

Overall, the SDI2 detected very similar growth patterns between the CR and DC polymers across both of the forces tested. A key observation was that at 5 kN, the CR polymer swelled to a slightly greater size than the DC polymer (Fig. 8 a and b). This correlated with the statistical findings from the independent *t*-test that overall the CR and DC polymers behaved similarly with the exception of 5 kN post 60 min which showed statistical difference.

From 20 min onwards for the compacts, the gel layer in the DC compact appeared to be less dense (especially for the 5 kN compacts). In contrast the CR polymer was denser for the same images (Fig. 7). This

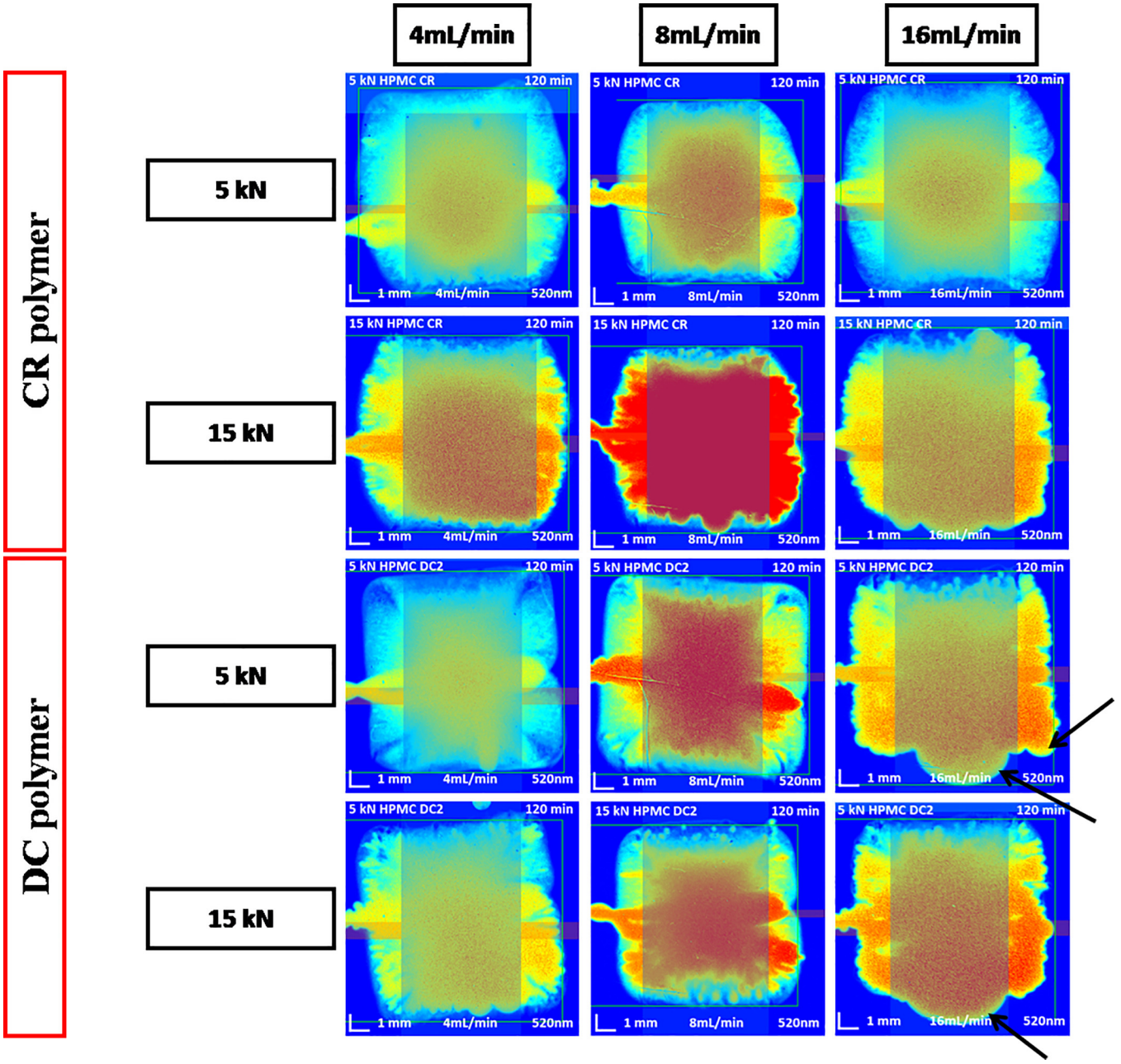

Fig. 6. False coloured SDI2 images for polymer compacts obtained from the SDI2 instrument at absorbance thresholds of 50 mAu for both the CR and DC polymer compacts at 5 and 15 kN at flow rates of 4, 8 and 16 mL/min. Note: The black arrows here indicate air bubbles lodged next to the compacts potentially giving erroneous results.

observation was in-keeping with similar differences detected by previous studies (Ervasti et al., 2015; Bonferoni et al., 1996). These studies suggested that polymers with fibrous morphology i.e. CR form denser gels due to the inter-locking and entanglement of the fibres and as a result may be able to control drug release more effectively. This observed difference was less pronounced as the compacts were subjected to increases in compaction force. This phenomenon can also be explained by the differences in porosity and solid fractions for the CR and DC polymers. DC had a solid fraction (converted into percentage) of 85% for the compact compacted at 5 kN whereas the CR had a solid fraction of 75% for the compact compacted at 5 kN suggesting that the more porous DC was bound to have a much higher ingress of water. The swelling data plot shown in Fig. 8, also displays the trends seen in the swelling images.

5. Conclusion

This novel work reports for the first time a method development for determining swelling of whole polymer compacts in real-time with high level of details under flow using a surface dissolution imaging instrument (SDI2). The results showed that overall, both polymers despite their differences in morphology swelled similarly at all the compaction forces tested. The growth rates of the DC compacts were inhibited despite its larger porosities as compared to the CR compacts resulting in the similarities seen between the two polymers. The methodology also detected other differences in the gel layers formed by both the DC and CR polymers indicating that the CR grade forms denser gels which could be attributed to the differences in the solid fraction. This novel work highlights an area of research that can provide a formulator insights into the behaviour of a range of formulations thereby informing

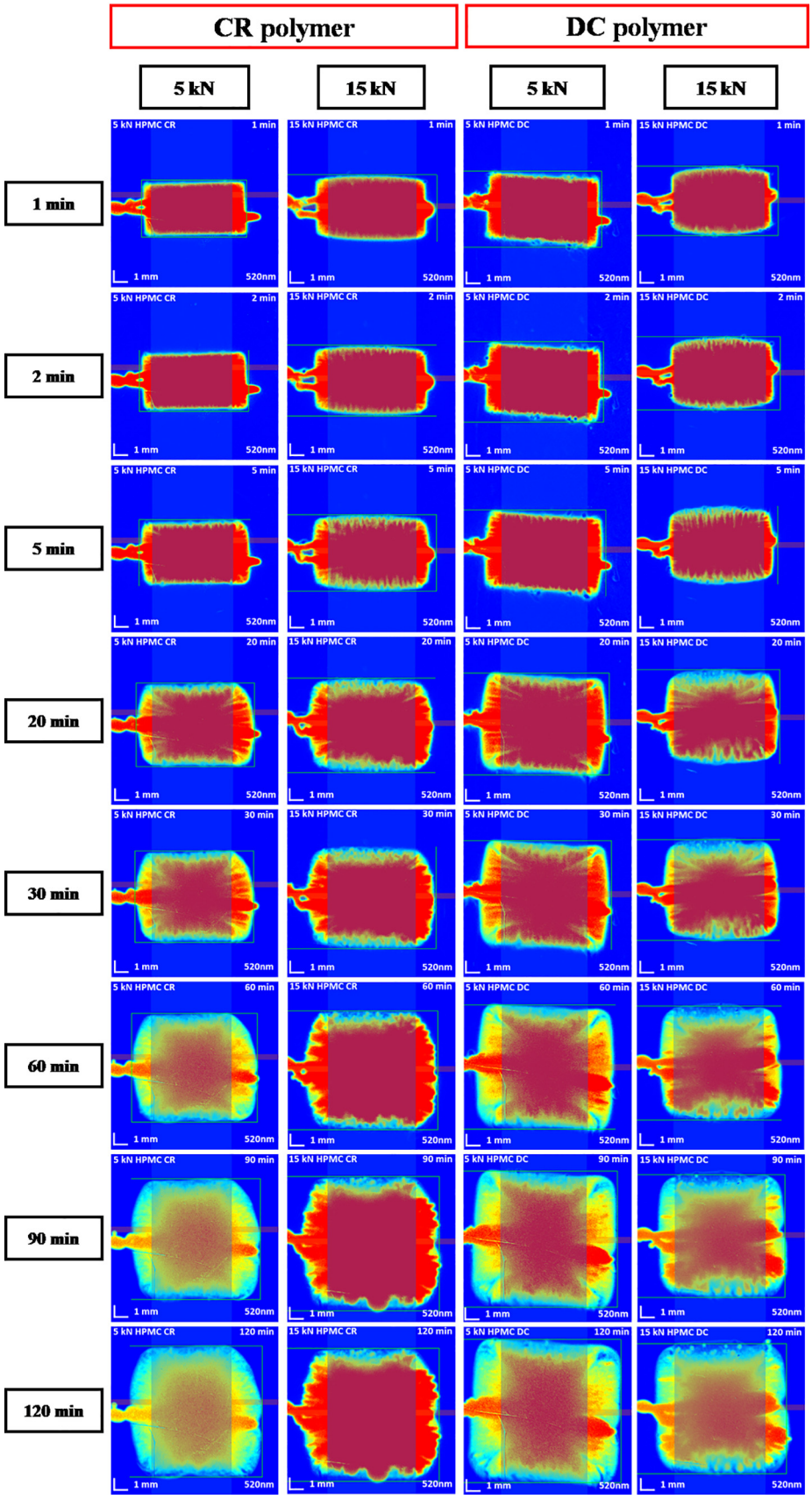

Fig. 7. False coloured SDI2 images of CR and DC polymers from time points 1 min to 120 min at two compressional levels (5 and 15 kN). Note: HPMC K100M CR is referred to as just CR in the manuscript whereas HPMC K100M DC is referred to as just DC in the manuscript.

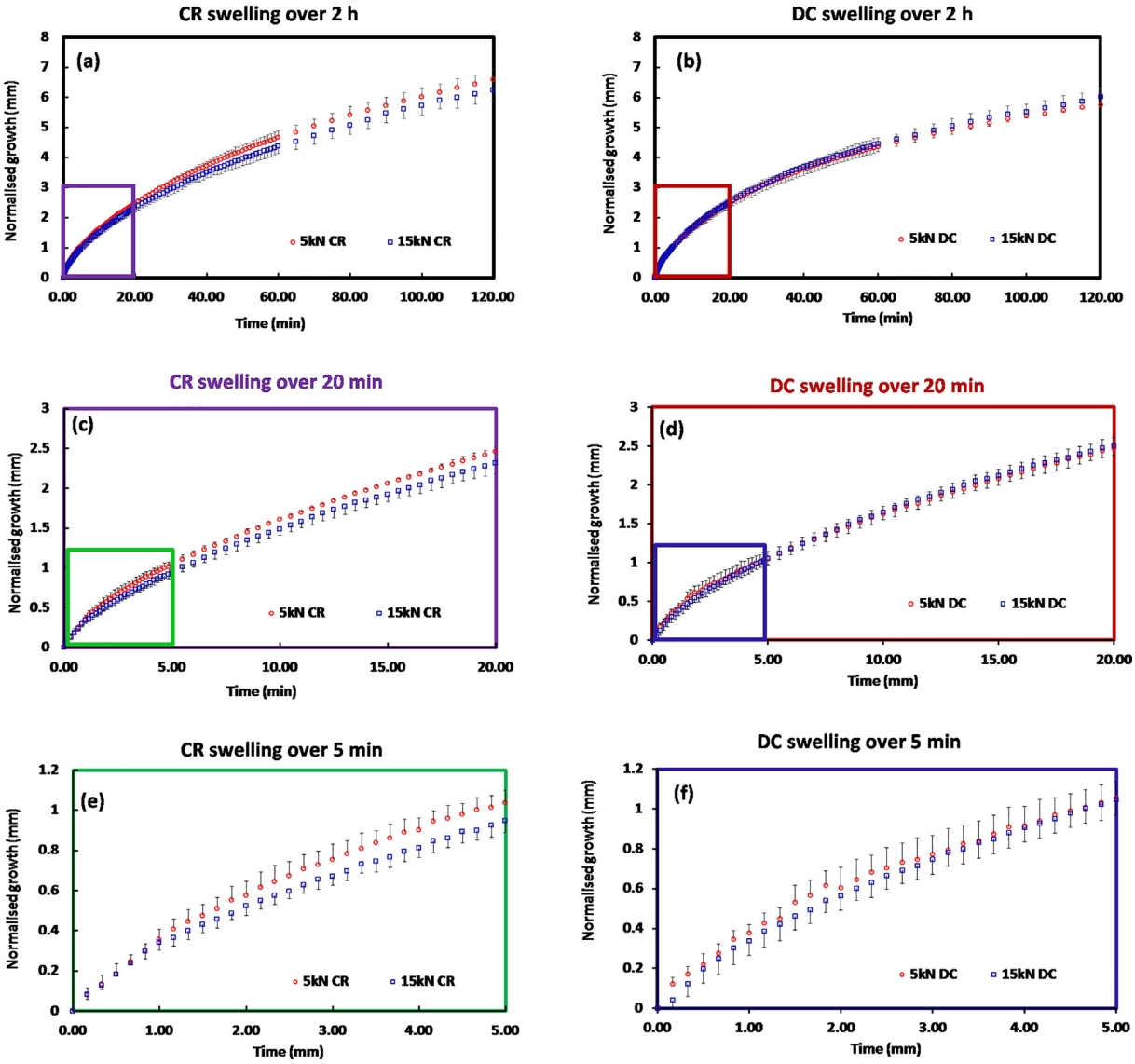

Fig. 8. Swelling data for polymer compacts obtained from the SDI2 instrument at a) 120 min for CR compacts at 5 and 15 kN compaction levels (purple box insert relates to Fig. 6c), b) 120 min for DC compacts at 5 and 15 kN compaction levels (red box insert relates to Fig. 6d), (c) 20 min for CR compacts at 5 and 15 kN compaction levels (green box insert relates to Fig. 6e), (d) 20 min for DC compacts at 5 and 15 kN compaction levels (blue box insert relates to Fig. 6f), (e) 5 min for CR compacts at 5 and 15 kN compaction levels and (f) 5 min for DC2 compacts at 5 and 15 kN compaction levels. Note: HPMC K100M CR is referred to as just CR in the manuscript whereas HPMC K100M DC is referred to as just DC in the manuscript. (For interpretation of the references to colour in this figure legend, the reader is referred to the web version of this article.)

decisions of choice of appropriate formulation for further investigation. However, care and consideration should be given to an appropriate selection of threshold absorbance used as this may potentially differ based on the nature of polymer tested.

Conflict of interest

The authors have no conflict of interest in the submitted work

Acknowledgements

The authors would like to thank the University of Huddersfield for funding Adam Ward. The authors are also grateful to Hayley Watson, Paul Whittles and Karl Box all of Sirius Analytical (now Pion) and to Hue Vuong , Kevin Hughes, Manish Ghimire and Ali Rajabi-Siahboomi all of Colorcon Ltd for the kind donation and manufacture of the compacts for this study. The authors also report no conflict of interest.

Appendix A. Supplementary data

Supplementary data to this article can be found online at https://doi.org/10.1016/j.ijpx.2019.100013.

References

Asare-Addo, K., Conway, B.R., Larhrib, H., Levina, M., Rajabi-Siahboomi, A.R., Tetteh, J., Nokhodchi, A., 2013a. The effect of pH and ionic strength of dissolution media on in-vitro release of two model drugs of different solubilities from HPMC matrices. Colloids Surf., B 111, 384–391.

Asare-Addo, K., Kaialy, W., Levina, M., Rajabi-Siahboomi, A., Ghori, M.U., Supuk, E., et al., 2013b. The influence of agitation sequence and ionic strength on in vitro drug release from hypromellose (E4M and K4M) ER matrices—The use of the USP III apparatus. Colloids Surf., B 104, 54–60.

Asare-Addo, K., Šupuk, E., Al-Hamidi, H., Owusu-Ware, S., Nokhodchi, A., Conway, B.R., 2015. Triboelectrification and dissolution property enhancements of solid dispersions. Int. J. Pharm. 485 (1), 306–316.

Asare-Addo, K., Walton, K., Ward, A., Totea, A.M., Taheri, S., Alshafiee, M., Conway, B.R., 2018. Direct imaging of the dissolution of salt forms of a carboxylic acid drug. Int. J.

Pharm. 551 (1–2), 290–299.
Asare-Addo, K., Alshafiee, M., Walton, K., Ward, A., Totea, A.M., Taheri, S., Timmins, P., 2019. Effect of preparation method on the surface properties and UV imaging of indomethacin solid dispersions. Eur. J. Pharm. Biopharm. 137, 148–163.
Ashraf, M., luorno, V.L., Coffin-Beach, D., Evans, C.A., Augsburger, L.L., 1994. A novel nuclear magnetic resonance (NMR) imaging method for measuring the water front penetration rate in hydrophilic polymer matrix capsule plugs and its role in drug release. Pharm. Res. 11 (5), 733–737.
Avalle, P., Pygall, S.R., Gower, N., Midwinter, A., 2011. The use of in situ near infrared spectroscopy to provide mechanistic insights into gel layer development in HPMC hydrophilic matrices. Eur. J. Pharm. Sci. 43 (5), 400–408.
Avalle, P., Pygall, S.R., Pritchard, J., Jastrzemska, A., 2013. Interrogating erosion-based drug liberation phenomena from hydrophilic matrices using near infrared (NIR) spectroscopy. Eur. J. Pharm. Sci. 48 (1), 72–79.
Boetker, J.P., Rantanen, J., Rades, T., Müllertz, A., Østergaard, J., Jensen, H., 2013. A new approach to dissolution testing by UV imaging and finite element simulations. Pharm Res 30 (5), 1328–1337.
Bonferoni, M.C., Rossi, S., Ferrari, F., Bertoni, M., Caramella, C., 1996. A study of three hydroxypropylmethyl cellulose substitution types: effect of particle size and shape on hydrophilic matrix performances. STP Pharm. Sci. 6 (4), 277–284.
Campos-Aldrete, M.E., Villafuerte-Robles, L., 1997. Influence of the viscosity grade and the particle size of HPMC on metronidazole release from matrix tablets. Eur. J. Pharm. Biopharm. 43 (2), 173–178.
Christmann, V., Rosenberg, J., Seega, J., Lehr, C., 1997. Simultaneous in vivo visualization and localization of solid oral dosage forms in the rat gastrointestinal tract by magnetic resonance imaging (MRI). Pharm. Res. 14 (8), 1066–1072.
Dinarvand, R., Wood, B., D'Emanuele, A., 1995. Measurement of the diffusion of 2,2,2-trifluoroacetamide within thermoresponsive hydrogels using NMR imaging. Pharm. Res. 12 (9), 1376–1379.
Ervasti, T., Simonaho, S., Ketolainen, J., Forsberg, P., Fransson, M., Wikström, H., et al., 2015. Continuous manufacturing of extended release tablets via powder mixing and direct compression. Int. J. Pharm. 495 (1), 290–301.
Haaser, M., Gordon, K.C., Strachan, C.J., Rades, T., 2013. Terahertz pulsed imaging as an advanced characterisation tool for film coatings—a review. Int. J. Pharm. 457 (2), 510–520.
Healy, A.M., Corrigan, O.I., Allan, J., 1995. The effect of dissolution on the surface texture of model solid-dosage forms as assessed by non-contact laser profilometry. Pharmaceut. Technol. Eur. 7, 14.
Heng, P.W.S., Chan, L.W., Easterbrook, M.G., Li, X., 2001. Investigation of the influence of mean HPMC particle size and number of polymer particles on the release of aspirin from swellable hydrophilic matrix tablets. J. Controll. Rel. 76 (1–2), 39–49.
Hu, A., Chen, C., Mantle, M.D., Wolf, B., Gladden, L.F., Rajabi-Siahboomi, A., et al., 2017. The properties of HPMC:PEO extended release hydrophilic matrices and their response to ionic environments. Pharm. Res. 34 (5), 941–956.
Hulse, W.L., Gray, J., Forbes, R.T., 2012. A discriminatory intrinsic dissolution study using UV area imaging analysis to gain additional insights into the dissolution behaviour of active pharmaceutical ingredients. Int. J. Pharm. 434 (1), 133–139.
Kaunisto, E., Abrahmsen-Alami, S., Borgquist, P., Larsson, A., Nilsson, B., Axelsson, A., 2010. A mechanistic modelling approach to polymer dissolution using magnetic resonance microimaging. J. Control. Rel. 147 (2), 232–241.
Khaled, S.A., Burley, J.C., Alexander, M.R., Yang, J., Roberts, C.J., 2015. 3D printing of five-in-one dose combination polypill with defined immediate and sustained release profiles. J. Control. Rel. 217, 308–314.
Kulinowski, P., Dorożyński, P., Młynarczyk, A., Węglarz, W.P., 2011. Magnetic resonance imaging and image analysis for assessment of HPMC matrix tablets structural evolution in USP apparatus 4. Pharm. Res. 28 (5), 1065–1073.
Levina M, Rajabi-Siahboomi A. An Industrial Perspective on Hydrophilic Matrix Tablets Based on Hyproxypropyl Methylcellulose (Hypromellose). 2014. pp. 53–85.
Li, C.L., Martini, L.G., Ford, J.L., Roberts, M., 2005. The use of hypromellose in oral drug delivery. J. Pharm. Pharmacol. 57 (5), 533–546.
Markl, D., Strobel, A., Schlossnikl, R., Bøtker, J., Bawuah, P., Ridgway, C., Zeitler, J.A., 2018. Characterisation of pore structures of pharmaceutical tablets: a review. Int. J. Pharm. 538 (1–2), 188–214.
Melia, C.D., Marshall, P., Stark, P., Cunningham, S., Kinahan, A., Devane, J., 1997. Investigating in vitro drug release mechanisms inside dosage forms. Adv. Exp. Med. Biol. 423, 129–135.
Nokhodchi, Ali, Raja, Shaista, Patel, Pryia, 2012. and Kofi Asare-Addo. The role of oral controlled release matrix tablets in drug delivery systems. BioImpacts: BI 2 (4), 175.
Østergaard, J., Meng-Lund, E., Larsen, S.W., Larsen, C., Petersson, K., Lenke, J., et al., 2010. Real-time uv imaging of nicotine release from transdermal patch. Pharm. Res. 27 (12), 2614–2623.
Pajander, J., Baldursdottir, S., Rantanen, J., Østergaard, J., 2012. Behaviour of HPMC compacts investigated using UV-imaging. Int. J. Pharm. 427 (2), 345–353.
Peltonen, L., Mannermaa, J., Yliruusi, J., 1997. Roughness analysis from tablet surfaces with a confocal laser scanning microscope. Pharmazie 52 (11), 860–863.
Pygall, S.R., Whetstone, J., Timmins, P., Melia, C.D., 2007. Pharmaceutical applications of confocal laser scanning microscopy: the physical characterisation of pharmaceutical systems. Adv. Drug Deliv. Rev. 59 (14), 1434–1452.
Rajabi-Siahboomi, A., Bowtell, R.W., Mansfield, P., Davies, M.C., Melia, C.D., 1996. Structure and behavior in hydrophilic matrix sustained release dosage forms: 4. Studies of water mobility and diffusion coefficients in the gel layer of HPMC tablets using NMR imaging. Pharm. Res. 13 (3), 376–380.
Siepmann, F., Karrout, Y., Gehrke, M., Penz, F.K., Siepmann, J., 2017. Limited drug solubility can be decisive even for freely soluble drugs in highly swollen matrix tablets. Int. J. Pharm. 526 (1–2), 280–290.
Sirius Analytical. Product Information – Sirius SDi2. 2017.
Tomer, G., Newton, J.M., Kinchesh, P., 1999. Magnetic resonance imaging (MRI) as a method to investigate movement of water during the extrusion of pastes. Pharm. Res. 16 (5), 666–671.
Timmins, P., Desai, D., Chen, W., Wray, P., Brown, J., Hanley, S., 2016. Advances in mechanistic understanding of release rate control mechanisms of extended-release hydrophilic matrix tablets. Therap. Deliv. 7 (8), 553–572.
Timmins, P., Pygall, S.R., Melia, C.D., 2014. Hydrophilic matrix tablets for oral. Control. Rel.
Van Snick, B., Holman, J., Cunningham, C., Kumar, A., Vercruysse, J., De Beer, T., et al., 2017. Continuous direct compression as manufacturing platform for sustained release tablets. Int. J. Pharm. 519 (1–2), 390–407.
Ward, A., Walton, K., Box, K., Østergaard, J., Gillie, L.J., Conway, B.R., et al., 2017. Variable-focus microscopy and UV surface dissolution imaging as complementary techniques in intrinsic dissolution rate determination. Int. J. Pharm. 530 (1), 139–144.
Yassin, S., Su, K., Lin, H., Gladden, L.F., Axel, Zeitler J., 2015. Diffusion and swelling measurements in pharmaceutical powder compacts using terahertz pulsed imaging. J. Pharm. Sci. 104 (5), 1658–1667.